

# Polymer complexes: supramolecular modeling for determination and identification of the bond lengths in novel polymer complexes from their infrared spectra<sup>1</sup>

Ahmed T. Mubarak<sup>1</sup>, A. Z. El-Sonbati<sup>1\*</sup>, A. A. El-Bindary<sup>1</sup>, R. M. Issa<sup>2</sup> and H. M. Kera<sup>2</sup>

<sup>1</sup>Department of Chemistry, Faculty of Science, King Khalid University, PO Box 9004, Abha 61413, Saudi Arabia

<sup>2</sup>Chemistry Department, Faculty of Science, Tanta University, Tanta, Egypt

Received 4 May 2006; Revised 29 July 2006; Accepted 3 August 2006

Synthesis and characterization of allyl propenyl-2-(4-derivatives phenylazo)butan-3-one (HL<sub>n</sub>) are described. The monomers obtained contain N=N and carbonyl functional groups in different positions with respect to the allyl group. This structural difference affects the stereochemical structure of the uranyl polymer complexes prepared by the direct reaction of uranyl acetate with the monomers. The polymer complexes are characterized by elemental analyses, <sup>1</sup>H and <sup>13</sup>C NMR, electronic and vibrational spectroscopy and other theoretical methods. The bonding sites of the hydrazone are deduced from IR and NMR spectra and each of the ligands were found to bond to the UO<sub>2</sub><sup>2+</sup> ion in a bidentate fashion. The monomers obtained contain N=N and carbonyl functional groups in different positions with respect to the allyl group. IR spectra show that the allyl azo homopolymer (HL<sub>n</sub>) acts as a neutral bidentate ligand by coordinating via the two oxygen atom of the carbonyl group, thereby forming a six-membered chelating ring. The  $\nu_3$  frequency of UO<sub>2</sub><sup>2+</sup> has been shown to be a good molecular probe for studying the coordinating power of the ligands. The  $\nu_3$ -values of UO<sub>2</sub><sup>2+</sup> from IR spectra have been used to calculate the force constant,  $F_{UO}$  (in 10<sup>-8</sup> N/Å) and the bond length  $R_{UO}$  (in Å) of the U–O bond. We adopted a strategy based upon both theoretical and experimental investigations. The theoretical aspects are described in terms of the well-known theory of 5d–4f transitions. The necessary structural data (coordination geometries and electronic structures) are determined from a framework for the modeling of novel polymer complexes. The Wilson, G. F. matrix method, Badger's formula and the Jones and El-Sonbati equations were used to determine the stretching and interaction force constants from which the U–O bond distances were calculated. The bond distances of these complexes were also investigated. The effect of Hamett's constant is also discussed. Copyright © 2006 John Wiley & Sons, Ltd.

**KEYWORDS:** supramolecular structures; UO<sub>2</sub><sup>2+</sup> azopolymer complexes; McGlynn and Badger's formula; Jones and El-Sonbati equations

## INTRODUCTION

The supramolecular assembly approach based on coordination compounds is primarily directed by the metal–ligand affinities, stereochemistries and substitution properties of the complexes involved. Another interesting property of

supramolecularly assembled polynuclear homopolymers is their ability to form homogeneous and adherent molecular films.

From the many interesting supramolecular systems that have been reported in the literature,<sup>1</sup> this study focuses mainly on a remarkable series of species constituted by homopolymers, uranium complexes, which has been systematically investigated in our laboratory for several years.<sup>2,3</sup> Molecular materials with unusual electric, magnetic or optical properties may be prepared from low-molecular-weight species capable of participating in supramolecular

\*Correspondence to: A. Z. El-Sonbati, Department of Chemistry, Faculty of Science, King Khalid University, P.O. Box 9004, Abha 61413, Saudi Arabia.

E-mail: elsonbatish@yahoo.com

<sup>1</sup>Abstracted from H.M. Kera's Ph.D. thesis.

structures.<sup>4</sup> We are interested in the synthesis and characterization of novel compounds containing 4-substituted phenylazoallylacetate ( $HL_n$ ) [Fig. 1(a)]. To our knowledge, no structures of azoallylacetate ( $HL_n$ ) transition metal polymer complexes have been reported in the literature.

Generally, the  $UO_2^{2+}$  cation adopts an octahedral geometry with the uranyl oxygen in the apical position. However, in the solid state, these materials can also be found as polymers that contain eight-coordinated uranium through oxygen atoms.<sup>2</sup> Such an interaction gives rise to a lowering of the  $U=O$  stretching frequency, which can be considered as a diagnosis of the actual uranium environment.<sup>5</sup> We are particularly interested in complexes that are able to enter into supramolecular associations through negatively charged groups on the ligand periphery.

The inspection of the molecular model structure of the above-mentioned compounds suggests that the characteristic ligands should possess a polymeric array in the solid state to create a rigid octahedral core. Accordingly, we have considered a series of ligands, such as the azoallyl derivatives ( $HL_n$ ) (Fig. 1) in which bis-coordination to  $UO_2^{2+}$  gives an octahedral geometry<sup>2</sup> structurally comparable to the above-mentioned azoquinolines.

The high polymer chemistry of  $HL_n$  has become increasingly important with considerable emphasis being placed on the chemistry and uses of organometallic derivatives.<sup>3,6</sup> The difference in reactivity of these heterocyclic materials and, unlike the *p*-derivative phenylazo group, their ability to induce protonation of the CH group [Fig. 1(a)] has been the subject of detailed investigations.<sup>7–9</sup> As part of our ongoing work<sup>2,3,6</sup> in the area of supramolecular assembly of polymer complexes based on aromatic amines, we report herein the synthesis, characterization and structure of  $HL_n$  and properties of the first example of hydrazone uranyl supramolecular polymer compounds  $[UO_2(HL_n)_2(OAc)_2]_n$  [see Fig. 1(b)] based on coordination, semicoordination and hydrogen bonds, which are of current interest due to their potential application related to inclusion phenomena, guest exchange and molecular-based uranium. Further studies are in progress involving other d- and/or f-metals and different stoichiometries in order to obtain a reasonable explanation and a better insight into this field of magnetic interactions.

## EXPERIMENTAL

### General procedure

Microanalysis of all samples was carried out at King Khalid University Analytical Center, Saudi Arabia, using a Perkin Elmer 2400 Series II Analyzer. The metal content in the polymer complexes was estimated by standard methods.<sup>3,4,10–15</sup> Infrared spectra were recorded as KBr pellets using a Pye Unicam Sp 2000 spectrophotometer.  $^1H$ - and  $^{13}C$ -NMR spectra were obtained on a JEOL Fx 900Q Fourier transform spectrometer with deuterated dimethylsulfoxide

(DMSO- $d_6$ ) as solvent and TMS as internal reference. The magnetic moment of the prepared solid complexes was determined at room temperature using the Gouy method. Mercury(II) tetrathiocyanatocobalt(II)  $[Hg\{Co(SCN)_4\}]$  was used for calibration of the Gouy tubes. Diamagnetic corrections were calculated from the values given by Selwood<sup>10</sup> and Pascal's constants.

### Synthesis of the ligands

Allylacetate, aniline and 4-*R*-aniline ( $R = OCH_3$ ,  $CH_3$ , Br and  $NO_2$ ; Aldrich Chemical Co.) were used without any further purification. The experimental technique has been described previously.<sup>2,3,8,9,11–15</sup>

### Preparation of allyl propenyl-2-(4-derivatives phenylazo) butan-3-one ( $HL_n$ )

In a typical preparation<sup>11–15</sup> 25 ml of distilled water containing hydrochloric acid (12 M, 2.68 ml, 32.19 mmol) were added to aniline (0.979, 10.73 mmol) or a 4-alkyl-aniline. The resulting mixture was stirred and cooled to 0 °C and a solution of sodium nitrite (740 mg, 10.73 mmol, in 20 ml of water) was added dropwise. The diazonium chloride that was formed was consecutively coupled with an alkaline solution of allylacetate, (0.142 mg, 10.73 mmol) in 20 ml pyridine. The resulting brown precipitate, which formed immediately, was filtered and washed several times with water. The crude product was purified by recrystallization from hot ethanol; yield 68%. The analytical data (Table 1) confirmed the expected compositions. The ligands were also characterized by  $^1H$ -NMR and IR spectroscopy.

### Synthesis of the polymer complexes

The uranyl salt,  $UO_2(CH_3COO)_2 \cdot 2H_2O$  (Aldrich Chemical Co.), was used as supplied. A 50 ml portion of a 0.5 M solution of the metal salt in *N,N*-dimethylformamide (DMF) was mixed with 50 ml of the monomer solution (0.1 M) in the same solvent and 0.1% w/v azobisisobutyronitrile (AIBN) as an initiator. The mixture was stirred under reflux for 6 h and the resulting polymer complexes were precipitated by addition to a large excess of distilled water containing hydrochloric acid to remove the excess metal salt. The precipitate was filtered, washed with water and dried in a vacuum oven at 40 °C for several days.

### Elemental analyses

The uranium content of each complex was determined by igniting a definite mass of the complex at 1000 °C and weighing the residue as  $U_3O_8$ . The analytical data are given in Table 1. The El-Sonbati equation was manipulated using a computer program developed in our laboratories using the C Language.

## RESULTS AND DISCUSSIONS

The ligands and metal polymer complexes under study are labeled as shown in Table 1 and Fig. 1. The elemental analyses

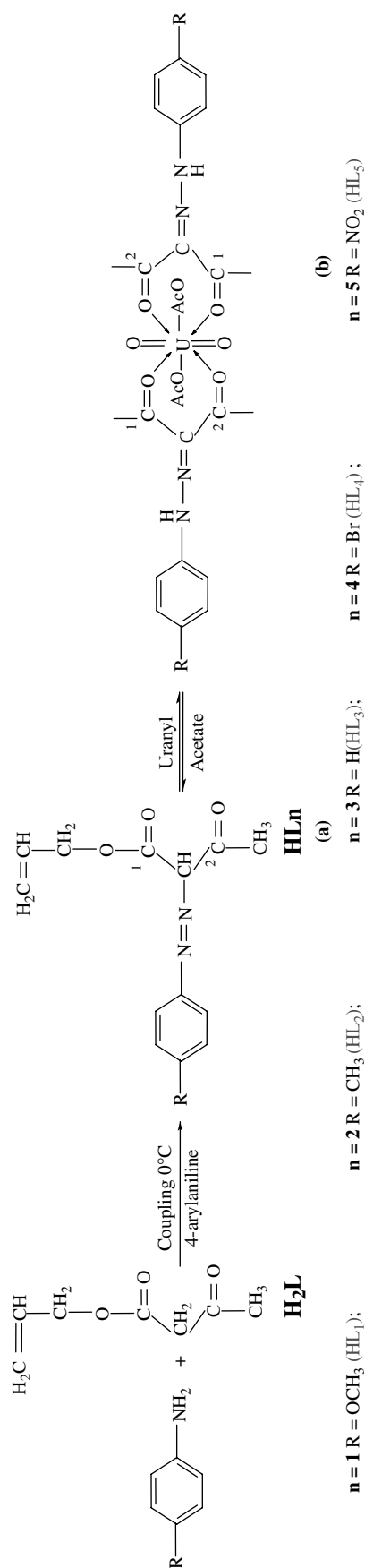
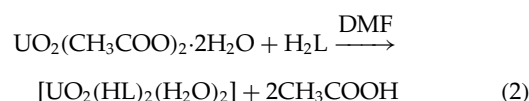
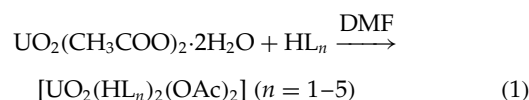


**Figure 1.** General formula and proton numbering scheme of the allyl propenyl-2-(4-derivatives phenylazo) butan-3-one ( $\text{HL}_n$ ).

of the six new polymeric complexes agree with the assigned formulae. The formation of the representative polymer complexes is summarized by equations (1) and (2), i.e. the polymer complexes were prepared by the reaction of the appropriate uranyl acetate with two equivalents of  $\text{HL}_n/\text{H}_2\text{L}$  in DMF. Liberation of hydrogen ions during complex formation was established by conductometric titration<sup>16</sup> of metal solution ( $10^{-3}$  M) in ethanol with a solution of ligand ( $5 \times 10^{-3}$  M) in the same solvent. The polymer complexes are microcrystalline or powder-like, stable under ambient conditions and are partially soluble in warm DMF and DMSO to varying extents. The polymer complexes do not melt but decompose on heating and are converted to  $\text{U}_3\text{O}_8$  around  $700^\circ\text{C}$ .<sup>9</sup> The molar conductivity in DMF indicates that the complexes are non-electrolytes.<sup>17</sup>



The magnetic measurements of the dioxouranium(VI) complexes are independent of field strength and temperature<sup>18</sup> and the ground states of dioxouranium(VI) compounds contain no unpaired electrons. The compounds are, therefore, weakly diamagnetic, as observed by previous workers.<sup>19</sup> Allyl propenyl-2-(4-derivatives phenylazo) butan-3-one ( $\text{HL}_n$ ) is a ligand whose reactivity toward metal ions varies as a function of the 4-substituents. The products, which are neutral, have two coplanar O,O metal-chelate rings in an O,O (O,O) *trans* geometry. Consequently, in the  $\text{UO}_2^{2+}$  case, the uranyl atom should be a six-coordinate octahedron with the oxygen atom in the apical position.<sup>8</sup> Bis(allyl propenyl-2-(4-derivative phenylazo)butan-3-one) uranyl has a low solubility in water and in common organic solvents. Therefore, in order to improve solubility, we have synthesized the azoallyl acetoacetate (Fig. 1), taking advantage of the high reactivity that diazonium salts exhibit with phenols.

## Characterization of the azo compounds

### $^1\text{H}$ NMR spectra

The  $^1\text{H}$  NMR data (Table 2) are in agreement with the proposed structures. The  $^1\text{H}$  NMR spectra of the ligand ( $\text{HL}_3$ ) and polymeric uranyl complex (3) supports the occurrence of the form depicted in Figs 1 and 2. A broad signal in compound 3 observed at 11.22 ppm is attributed to the NH proton. A high field is seen for the CH resonance of the ligand, which appears as a singlet at  $\delta$  3.61 ppm; the last two protons disappear in the presence of  $\text{D}_2\text{O}$ . Further, the CH signal vanishes and a new NH and C=N signal appears upon complexation, i.e. a change from azo to hydrazo form. The aromatic protons have resonances at 7.1–7.45 ppm for the ligand. Chelation causes a downfield shift of  $\sim 0.7$  ppm. The characteristic proton

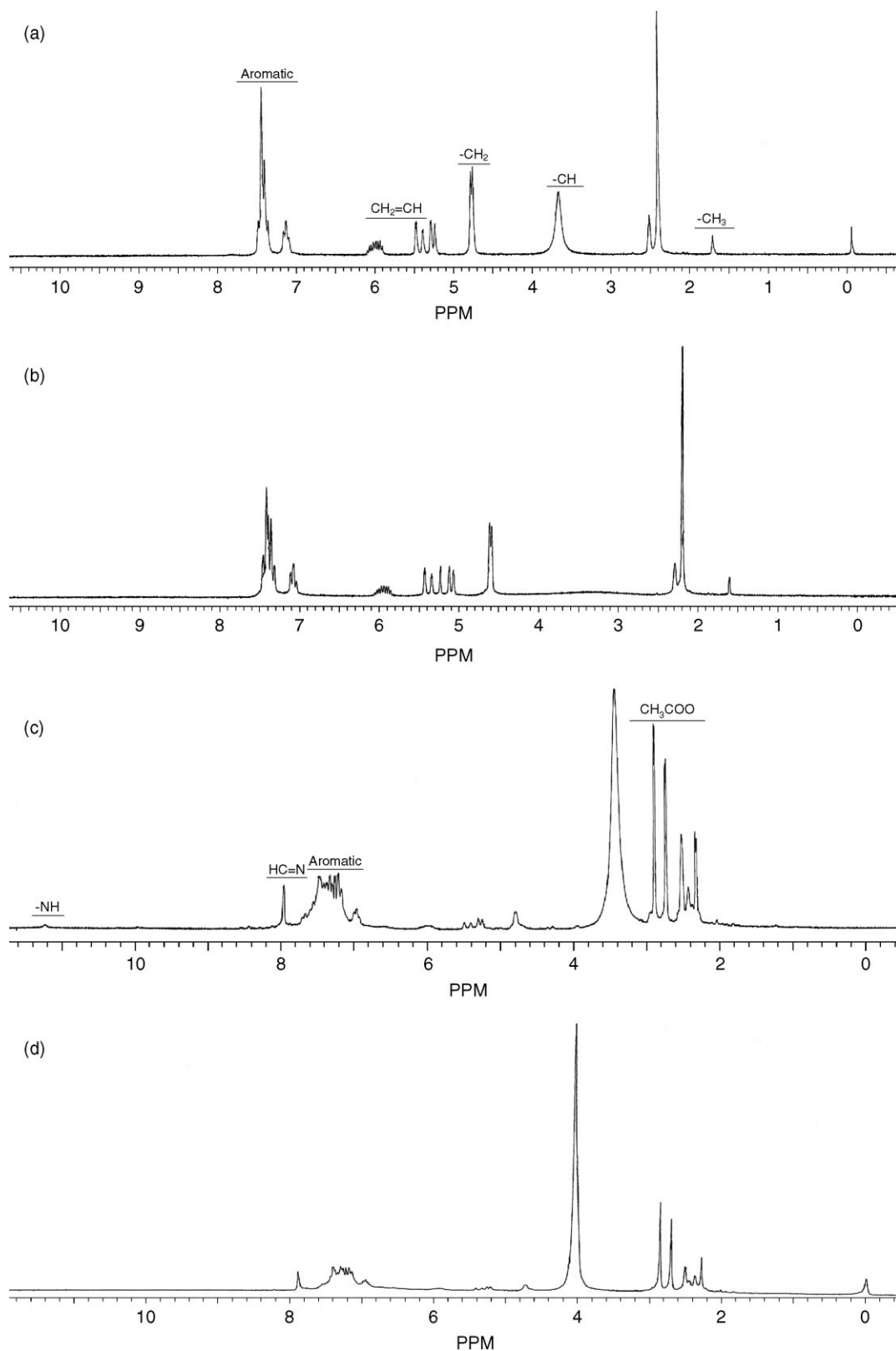


**Figure 2.**  $^1\text{H}$  NMR chemical shift ( $\text{DMSO-d}_6$ ) (ppm vs TMS): (a)  $\text{HL}_3$ ; (b)  $\text{HL}_3$  with  $\text{D}_2\text{O}$ . (c) Compound **3** and (d) compound **3** with  $\text{D}_2\text{O}$ .

**Table 1.** Analytical data for  $\text{UO}_2^{2+}$  polymer complexes<sup>a</sup> of allyl propenyl-2-(4-derivatives phenylazo) butan-3-one ( $\text{HL}_n$ ) [for molecular structures see Fig. 1(a, b)]<sup>b</sup>

Compound <sup>c</sup>		Experimental (calculated) (%)				Composition
Colour	Code	C	H	N	Metal	Colour
HL <sub>1</sub>	1	61.0	5.7	10.4	—	$[\text{UO}_2(\text{HL}_1)_2(\text{OAc})_2]_n$ Dark brown
Brown		(60.9)	(5.8)	(10.2)		
		41.0	4.1	6.2	25.6	
		(40.9)	(4.0)	(6.0)	(25.3)	
HL <sub>2</sub>	2	64.5	6.1	11.0	—	$[\text{UO}_2(\text{HL}_2)_2(\text{OAc})_2]_n$ Dark brown
Orange		(64.6)	(6.2)	(10.8)		
		42.2	4.3	6.5	26.5	
		(42.3)	(4.2)	(6.2)	(26.2)	
HL <sub>3</sub>	3	63.5	5.6	11.6	—	$[\text{UO}_2(\text{HL}_3)_2(\text{OAc})_2]_n$ Brown
Orange		(63.4)	(5.7)	(11.4)		
		41.0	4.0	6.6	26.8	
		(40.9)	(3.9)	(6.4)	(27.1)	
HL <sub>4</sub>	4	47.9	3.9	8.8	—	$[\text{UO}_2(\text{HL}_4)_2(\text{OAc})_2]_n$ Dark brown
Pale orange		(48.0)	(4.0)	(8.6)		
		34.7	3.0	5.7	23.2	
		(34.7)	(3.1)	(5.4)	(22.9)	
HL <sub>5</sub>	5	53.5	4.6	14.6	—	$[\text{UO}_2(\text{HL}_5)_2(\text{OAc})_2]_n$ Pale yellow
Yellow		(53.6)	(4.5)	(14.4)		
		37.0	3.4	8.9	24.7	
		(37.1)	(3.3)	(8.7)	(24.5)	

<sup>a</sup> Microanalytical data as well as metal estimations are in good agreement with the stoichiometry of the proposed complexes.

<sup>b</sup> The excellent agreement between calculated and experimental data supports the assignment suggested in the present work.

<sup>c</sup>  $\text{HL}_1$ – $\text{HL}_5$  are the monomer and azomonomer as given in Fig. 1(a).

resonances of the substituted and unsubstituted and benzene ring of the ligand and other polymer complexes are almost unchanged.

The  $^1\text{H}$  NMR spectrum of the  $\text{HL}_3$  monomer showed the expected peaks and pattern of the vinylic group ( $\text{CH}_2 = \text{CH}$ ), i.e.  $\delta$  (DMSO- $d_6$ ) 6.36 (dd,  $J = 17, 11$  Hz) for the vinyl CH proton and  $\delta$  5.21 ppm (AM part of AMX system dd,  $J = 17, 11$  Hz, and dd,  $J = 11, 1$  Hz) for the vinyl  $\text{CH}_2$  protons, respectively. These peaks disappeared on polymerization while a triplet at  $\delta$  1.98 (t,  $J = 7$  Hz) and a doublet at  $\delta$  1.86 ppm (d,  $J = 7$  Hz) appeared. This indicates that the polymerization of  $\text{HL}_3$  monomer occurs on the vinyl group. It is worth noting that the rest of the proton spectra of the monomer and polymer remain almost unchanged.

The  $^{13}\text{C}$  NMR data (Table 2) related to both the free ligand ( $\text{HL}_3$ ) and the uranyl complex (3) are obtained for the related symmetrical species. The assignments are made based on  $^1\text{H}$ -coupled spectra and chemical shift values.



The  $^{13}\text{C}$  NMR spectra give information about the carbon skeleton of the molecule. Assignment of different resonance peaks to respective carbon atoms are presented in Table 2 and Fig. 1, considering the two carbonyl oxygens as non-equivalent. In both, the  $\text{C}_1$  and  $\text{C}_2$  carbon atoms adjacent to the more electronegative nitrogen atom of azodye group

in the ligand [Fig. 1(a)] and the hydrazone group in the case of the polymer complex [3, see Fig. 1(b)] are shifted further downfield when compared with the neighboring carbon atoms. Also, the carbon atoms at the *para* position of the aromatic carbon resonate at lower field values when compared with the  $\text{C}_1$  and  $\text{C}_2$  of  $\beta$ -allyl diketonate. However, the non-protonated carbons show more downfield shift in the side chain due to an increased electron density resulting from the presence of electronegative nitrogen and/or oxygen atoms and  $\pi$ -electron delocalization in the magnetic environment. In the proton-decoupled  $^{13}\text{C}$  NMR spectrum of compound 3, the carbon resonance of the azomethine group [see Fig. 1(b)], adjacent to the allyl  $\beta$ -diketonate group, is found at  $\delta = 150.3$  ppm.

The effects of complexation may be deduced from a comparison throughout the series of symmetrical compounds. As expected the C-1 [ $\text{C}-1$  of monomer = 194.8 and C-2 of uranyl complex = 177.3] and the C-2 nuclei [ $\text{C}-2$  of monomer = 194.4 and C-2 of uranyl complex = 176.9] are the most affected.

As previously mentioned, the large differences observed between the chemical shift of similar carbons in the symmetrical complexes and the free ligand  $\text{HL}_n$  have been attributed to the inductive effect of the methoxy group.<sup>20</sup>

**Table 2.**  $^1\text{H}$  and  $^{13}\text{C}$  NMR chemical shift (ppm vs TMS)<sup>a</sup>

Compound	Group	$^1\text{H}$ -NMR (ppm) <sup>b</sup>	$^{13}\text{C}$ -NMR (ppm) <sup>c</sup>
HL <sub>3</sub>	CH <sub>2</sub> =CH	6.0 5.4	122.2 139.0
	CH <sub>2</sub>	4.8	68.0
	CH <sub>3</sub>	1.85	13.9
	CH	3.61	109.8
		7.1–7.45	110–140.0
	C-1		194.8
	C-2		194.4
Complex 3	CH <sub>2</sub> -CH	6.21 5.3	65 55
	CH <sub>2</sub>	4.8	68.3
	CH <sub>3</sub>	2.21	14.1
		6.95–7.5	117.3–137.0
			
	C=N	7.95	150.3
	NH	11.22	
	C-1		177.3
	C-2		196.9

<sup>a</sup> The agreement experimental data supports the assignment suggested in the present work.

<sup>b</sup> See Figs 1 and 2;

<sup>c</sup> see Fig. 1.

Furthermore, the chemical shift differences are much smaller in the free ligand than in the uranyl polymer complex, suggesting the polarizing influence of the metal center.

Finally, both the  $^1\text{H}$  and  $^{13}\text{C}$  NMR spectra provide strong support for the bonding characteristic of the HL<sub>n</sub> in forming polymer complexes with UO(II) ion through the two carbonyl oxygen atoms.

### Infrared spectra and nature of coordination

By tracing the IR spectra of the uncomplexed azo, no  $\nu\text{NH}_2$  stretching vibrations are apparent. This supports the formation of azodye ligands. The mode of bonding of the HL<sub>n</sub> to the metal ions was elucidated by comparing the IR

spectra of the polymer complexes with literature data for related systems.

The spectra exhibit a medium to strong band in the region 1400–1500  $\text{cm}^{-1}$ , which could be assigned to  $\nu\text{N}=\text{N}$  stretching vibration.<sup>2</sup> The C=C stretching vibrations of the phenyl ring at 1500–1600  $\text{cm}^{-1}$  are due to the symmetric and asymmetric vibrations, respectively (Table 3).

The strong bands located at 1690–1640  $\text{cm}^{-1}$  due to carbonyl stretching vibrations modes are expected to occur in this region. Several authors<sup>21,22</sup> have confirmed the existence of these carbonyl groups, where the highest frequency band is assigned to the CO symmetric stretch while the lowest frequency band is due to CO antisymmetric stretch, respectively. The two bands in the 1600–1500  $\text{cm}^{-1}$  region are characteristic of the six-membered ring system formed. The region between 1500 and 900  $\text{cm}^{-1}$  is due to C–N stretching and out-of-plane C–H bending vibrations. The symmetric and antisymmetric C=C stretching modes are expected to exist in this region.

In general, the presence of electron attracting group minimizes the charge transfer from the phenyl ring and this leads to increased the CO band intensity. The three bands located at 2995, 2960 and 2860  $\text{cm}^{-1}$  are a strong indication of the presence of a methoxy group (HL<sub>1</sub>). The strong bands at 1530 and 1490  $\text{cm}^{-1}$  support the presence of  $\nu(\text{N}=\text{N})$ . The  $\beta\text{C}-\text{H}$ ,  $\delta\text{C}-\text{H}$  and  $\gamma\text{C}-\text{H}$  modes of vibrations are identified by the presence of strong bands in the ranges 1180–1110, 1030–930 and 840–780  $\text{cm}^{-1}$ , respectively. The C–C vibrations are also identified by the presence of several bands at frequencies lower than 755  $\text{cm}^{-1}$ . Generally, the electron donor methoxy group enhances the charge transfer from the phenyl ring to the heterocyclic moiety. This leads to increase in polarizability of the carbonyl group. The methyl group attached to aromatic rings have been studied in detail by several authors.<sup>23,24</sup> A large number of hydrocarbons containing methyl groups gave two strong bands at 2960 and 2870  $\text{cm}^{-1}$ , corresponding to asymmetric and symmetric C–H stretching modes of vibration, respectively. The three bands located at  $\sim 1490$ ,  $\sim 1450$  and  $\sim 1420$   $\text{cm}^{-1}$  are due to

**Table 3.** Selected IR spectral data ( $\text{cm}^{-1}$ ) of the free ligand and uranyl polymer complexes [for molecular structures see Fig. 1(a, b)]

Compound <sup>a</sup>	Frequency ( $\text{cm}^{-1}$ )					
	$\nu\text{C}=\text{N}$	$\nu\text{-NH}$	$\nu\text{C}-\text{O}-\text{C}$	$\nu\text{C}=\text{O}$	$\nu\text{N}=\text{N}$	$\nu\text{C}=\text{C}^b$
Ligands	—	—	1080	1690–1640	1485–1445	1660–1630
1	1625	3340	1083	1680	—	—
2	1620	3280	1083	1665	—	—
3	1618	3260	1083	1660	—	—
4	1610	3215	1081	1640	—	—
5	1615	3245	1083	1655	—	—
6	—	—	1081	1635	—	—

<sup>a</sup> The serial number corresponds to that used in Table 1 and Fig. 1(b).

<sup>b</sup> Acrylic double bond.

methyl deformation for C–H bending absorption expected to be present in the ligand (HL<sub>2</sub>).

The free ligand exhibits a strong broad due to the carbonyl groups attached to the allyl group in the region 1690–1640 cm<sup>-1</sup> and at 1080 cm<sup>-1</sup> due to  $\nu(\text{C}=\text{O})$ .<sup>24</sup> In the IR spectra of the corresponding uranyl polymer complexes, the broad band changed and the band at 1080 cm<sup>-1</sup> appeared almost in the same region. This suggests that the bonding takes place through the carbonyl groups to the UO<sub>2</sub><sup>2+</sup> ion.

A study and comparison of infrared spectra of free ligands and their UO<sub>2</sub><sup>2+</sup> polymer complexes (Table 2) imply that these ligands behave as neutral bidentate donors to the UO<sub>2</sub><sup>2+</sup> coordinated through the O,O of the two carbonyl groups. The strong broad bands observed in the 1690–1640 cm<sup>-1</sup> region in the free ligand have been assigned to  $\nu(\text{CO})$  vibrations. Hence, upon complexation, these frequencies were observed to be shifted to lower wavenumber (Table 2) and the intensities of the bands are also reduced. The absorption bands at 3340–3215 and at  $\sim 1620 \pm 5$  cm<sup>-1</sup> after complexation have been assigned to  $\nu(\text{NH})$  and  $\nu(\text{C}=\text{N})$ , respectively.

The possibility of azo-hydrazone tautomerism in these ligands has been ruled out since no bands around 3500 and 1630 cm<sup>-1</sup>, characteristic of  $\nu(\text{OH})$  and  $\delta(\text{OH})$  groups, are displayed in the infrared absorption. The three fundamental modes of vibrations of the UO<sub>2</sub><sup>2+</sup> ion are IR active in the present polymer complexes which explain the linearity of the uranyl entity.<sup>6,23</sup> The  $\nu(\text{C}=\text{O})$  of the acetate in the uranyl polymer complexes is probably merged with the band of the carbonyl groups present in the IR spectra of the complexes.

It is known that  $\beta$ -diketonate vibrations, especially with frequencies lower than  $\sim 700$  cm<sup>-1</sup>, are not characteristic because of strong delocalization of  $\pi$ -electron density. M–O bonds with participation of chelate ring deformation and the radicals give the most substantial contribution to vibrations in the region 400–700 cm<sup>-1</sup>. Participation of the  $\nu(\text{C}\dots\text{O})$ ,  $\nu(\text{C}\dots\text{C})$  bonds increases in vibrations with frequencies higher than 1000 cm<sup>-1</sup>. Increasing the  $\pi$ -electronic density in a chelate ring correlated with decreasing the effective charge on oxygen atoms and lowered the strength of the U–O bonds.

## Spectroscopic studies

HL<sub>n</sub> exhibits bands four bands within the regions: A (24 980–23 255 cm<sup>-1</sup>), B (34 460–33 890 cm<sup>-1</sup>), C (36 360–35 700 cm<sup>-1</sup>) and D (40 990 cm<sup>-1</sup>). According to previously reported results<sup>8</sup> on similar compounds, the two bands C and D are assigned to phenyl transitions ( $\text{ph}-\text{ph}^*$ ,  $\pi-\pi^*$ ). Band B is assigned to the carbonyl (CO) and azo (N=N) groups and the phenyl ring transitions ( $n-\pi^*$ ,  $\pi-\pi^*$ ). The absorption band observed within the wavelength A arises from a transition involving electron migration along the entire conjugate system of the ligands, i.e. it comprises charge transfer (CT) from the substituted phenyl ring to the carbonyl groups by resonance and from the phenyl ring by induction. This latter assumption is substantiated by the fact that this band is highly influenced by the nature of the substituent R. The donor substituents cause a red

shift relative to the unsubstituted derivative (H) in the order OCH<sub>3</sub> > CH<sub>3</sub> > H > Cl > NO<sub>2</sub>. The R-phenyl moiety acts as an electron acceptor conjugated system and the CT takes place between these two centers.<sup>25</sup>

In the case of bromo and nitro derivatives,  $\lambda_{\text{max}}$  is more or less similar to that of the unsubstituted compound. This behavior can be ascribed to antagonistic effect viz. mesomeric and inductive effects.

## Complexation effect on uranyl ion spectra

Substituent effects on reactivities depend mainly on the rate-controlling step and the nature of the transient species. Hamett's equation related the reactivity trends in ligands and complexes to the stability, i.e. the lower the stability the higher the reactivities. Based on Hamett's relationship, electron-withdrawing substituents to ligands in their complexes enhance the stabilities of these complexes owing to the decrease in electron density at the metal central atom and thus the increase in the positive charge on the metal. Therefore, this effect results in decreasing reactivity. In contrast, electron-donating substituents increase the electron density at the metal and leading to decrease the stability of the metal chelates

The uranyl ion UO<sub>2</sub><sup>2+</sup> is quite characteristic in its own structure and in its coordination compounds.<sup>3,24,26</sup> The ion retains its identity over a wide range of vibrations in experimental conditions and can be considered from the geometric point of view, as a single particle. In the present investigation, the  $\nu(\text{U}=\text{O})$  in all complexes has been assigned as 925–900 cm<sup>-1</sup> ( $\nu_3$ ) and 818–791 cm<sup>-1</sup> ( $\nu_1$ ) (Table 4). The  $\nu_3$  values decrease as the donor characteristic increase, as observed for  $\pi$ -electron substituents, where the basicity of the donating atom increases.

In the equatorial bonding the more effective overlap of the O–U–O group orbital by oxygen–oxygen orbitals in the ligands leads to lower  $\nu_3$  values for UO<sub>2</sub><sup>2+</sup> complexes.<sup>3,27</sup> The phenomenon is also observed in the present uranyl complex, where the number of donor ligands in the equatorial plane increases. A group theoretical consideration<sup>28</sup> shows that a linear and symmetrical triatomic UO<sub>2</sub><sup>2+</sup> ion possessing *D*<sub>∞h</sub> symmetry gives rise to three fundamental modes of vibrations.

Although the change in  $\nu_3(\text{UO}_2)$  observed in the present uranyl polymer complexes is comparable with those observed by Paolucci *et al.*,<sup>29</sup> a clear-cut correlation is not possible in these species as the coordination in the equatorial plane is almost similar in these complexes.

The experimental results reveals a linear relation between  $\nu_1$  and  $\nu_3$  with the slope corresponding to  $(1 + 2M_{\text{O}}/M_{\text{U}})^{1/2}$ , where *M*<sub>O</sub> and *M*<sub>U</sub> are the masses of oxygen and uranium atoms respectively [Fig. 3(a)]. Similar results have been reported by McGlynn and Smith.<sup>30</sup> It is clear that good linearity is obtained also in case of  $\nu_1'$  and  $\nu_3'$  (Fig. 4).

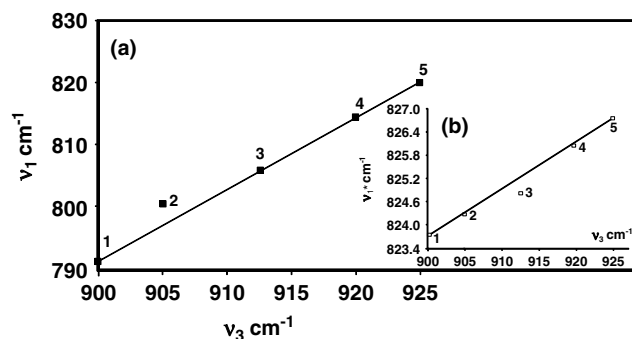
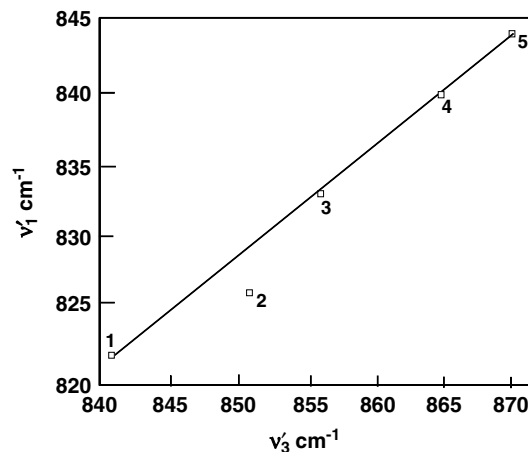
Instead of the linear relation between  $\nu_1$  and  $\nu_3$  frequencies, the El-Sonbati equation<sup>31</sup> has focused attention on their

**Table 4.** Various force constants ( $10^{-8}\text{N}/\text{\AA}$ ), U–O bond distances ( $\text{\AA}$ ) and frequencies ( $\text{cm}^{-1}$ )  $\nu_1$  and  $\nu_3$  of the isolated  $\text{UO}_2^{2+}$  polymer complexes [for molecular structure see Fig. 1(b)]

Serial no. <sup>a</sup>	$\nu_1$	$\nu_1'$	$\nu_3$	$\nu_3'$	$F_{\text{UO}}$	$r_1$	$r_2$	$(F_{\text{S-U-O}})_{\text{t}}$	$r_{\text{t}}$	$(F_{\text{S-U-O}})_{\text{o}}$	$r_0$	Percent- tage error	$(F_{\text{UO,UO}})^{\text{b}}$	$(\nu_1^*)^{\text{c}}$	$F_{\text{X-U-O}}$	$r_3$	$(F_{\text{UO,UO}})^{\text{b}}$	$w_3$	$w_1$	$(r_3 - r_1)^2$	$(r_1 - r_t)^2$	$(r_2 - r_t)^2$
1	791	822	900	841	6.6858	1.7433	1.7239	5.9282	1.7667	5.8379	1.7698	1.5	0.7636	823.9	6.1476	1.7596	0.5444	907.8	802.2	$5.041 \times 10^{-5}$	$5.4756 \times 10^{-4}$	$1.83184 \times 10^{-3}$
2	800	826.5	905	851	6.7603	1.7412	1.7200	6.0246	1.7635	5.9776	1.7651	0.78	0.7418	824.2	6.1866	1.7583	0.5802	912.8	811.2	$2.704 \times 10^{-5}$	$4.9729 \times 10^{-4}$	$1.89225 \times 10^{-3}$
3	805	832.7	912	856.4	6.8653	1.7383	1.7146	6.1100	1.7608	6.0537	1.7626	0.92	0.7612	824.8	6.2436	1.7565	0.6276	919.8	816.2	$1.849 \times 10^{-5}$	$5.0625 \times 10^{-4}$	$2.13444 \times 10^{-3}$
4	813	839.8	920	864.9	6.9862	1.7350	1.7085	6.2241	1.7571	6.1745	1.7587	0.80	0.7683	826.0	6.3123	1.7544	0.6803	927.8	824.2	$7.29 \times 10^{-6}$	$4.8841 \times 10^{-4}$	$2.36196 \times 10^{-3}$
5	818	844.3	925	870	7.0624	1.7329	1.7048	6.2958	1.7549	6.2475	1.7564	0.77	0.7728	826.8	6.3560	1.7530	0.7128	932.8	829.2	$3.61 \times 10^{-6}$	$4.84 \times 10^{-4}$	$2.51001 \times 10^{-3}$
																				$\sqrt{1.0684} \times 10^{-4} =$	$\sqrt{2.52351} \times 10^{-3} =$	$\sqrt{0.0107305} =$
																				0.0103363	0.05023450	0.1035881

<sup>a</sup> The serial number corresponds to that used in Table 1 and Fig. 1(b).<sup>(1,2)</sup> Internuclear distance U–O calculated by using the Badger equation and the Jones equation.<sup>b</sup> U–O force constant and  $\text{UO}_2^{2+}$  interaction constant with neglect of the interaction of the UO bonds with the ligands,  $(F_{\text{UO, UO}} = \text{bond-bond interaction})$ .<sup>c</sup> Symmetric stretching frequency evaluated using the El-Sonbati equation.

$(\nu_1', \nu_3')$  is the symmetric and asymmetric stretching frequency with neglect of the ligands.  $(F_{\text{U-O}})_{\text{t}}$  is the true value of the force constant.  $(F_{\text{U-O}})_{\text{o}}$  is the constant calculated with neglect of the ligands.  $F_{\text{U-O}}$  is the band force constant evaluated using the El-Sonbati equation.  $r_{\text{t}}$  is the internuclear distance U–O calculated using the true value of the force constant.  $r_0$  is the internuclear distance U–O calculated using the asymmetric stretching frequency with neglect of the ligands.  $r_3$  is the internuclear distance U–O calculated using the symmetric stretching frequency evaluated using the El-Sonbati equation.

**Figure 3.** The relation between (a)  $\nu_1$  vs  $\nu_3$  and (b)  $\nu_1^*$  vs  $\nu_3$ .**Figure 4.** The relation between  $\nu_1'$  vs  $\nu_3'$ .

normalized differences (Fig. 5):

$$\frac{(\nu_1^2 + \nu_3^2)}{\nu_1 \nu_3} = A \nu_3 + B \quad (3)$$

With slope  $A(0.000192)$  and constant  $B(1.835)$ , correlation does not depend on the masses of the oxygen and/or uranium atoms. We have made qualitative studies on the present uranyl complexes and in most cases it is easy to observe and assign the fundamental frequency  $\nu_3$  and the combination frequency  $\nu_1 + \nu_3$  (Fig. 6). There is also a straight line relationship between  $w_1$  and  $w_3$  (Table 4) and Fig. 7. However, the rest of the spectrum is generally complex and it may not be possible to determine the remaining fundamental frequencies.

Our objective is using the El-Sonbati equation from which the U–O bond force constant should eventually serve as a fairly accurate measure of the U–O bond distance in given compounds. The force constant for the U–O bond  $[F_{\text{U-O}} 10^{-8}\text{N}/\text{\AA}]$ ,  $(F_{\text{U-O}})_{\text{t}}$ ,  $(F_{\text{U-O}})_{\text{o}}$  and  $F_{\text{UO, UO}}$ , neglecting the interaction of the U–O bonds with the ligands, the U–O bond distance ( $r_{\text{U-O}} \text{\AA}$ ) and spectral data used herein are presented in Table 4. It is apparent from Table 4 that a plot of  $\nu_1 + \nu_3$



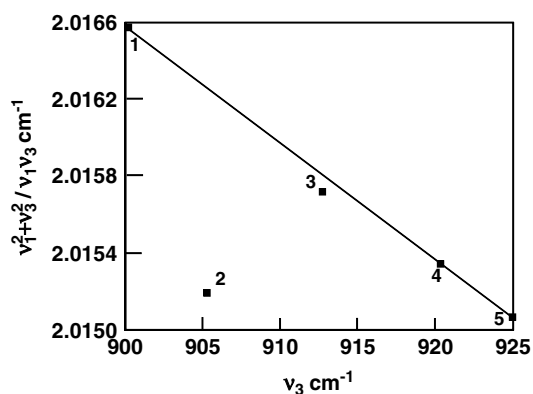


Figure 5. The relation between  $v_1^2 v_3^2 / v_1 v_3$  vs  $v_3$ .

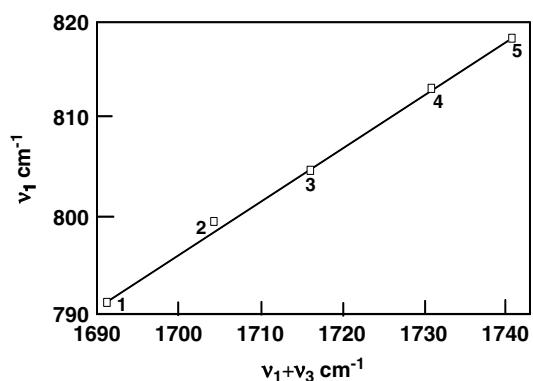


Figure 6. The relation between  $v_1$  and  $v_1 + v_3$ .

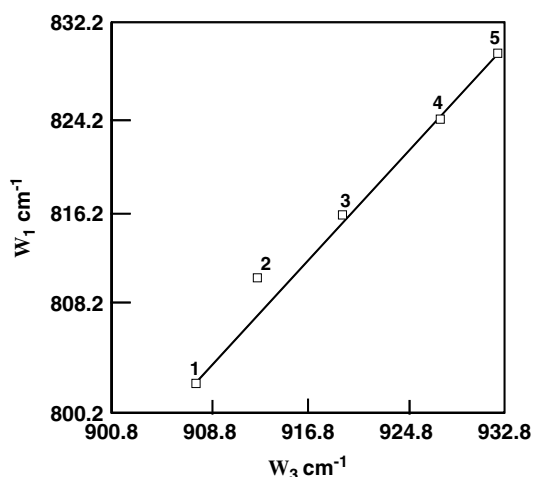


Figure 7. The relation between  $w_1$  vs  $w_3$ .

and/or  $v_3$  vs force constant for the U–O ( $F_{U-O}$   $10^{-8}$  N/Å or  $F_{U-O}^*$   $10^{-8}$  N/Å) and the U–O bond distance ( $r_{U-O}$  Å or  $r_{3U-O}$  Å) gives a straight line with an increase in the value of  $v_1 + v_3$  and/or  $v_3$  decrease  $r_{U-O}$  and an increase in the

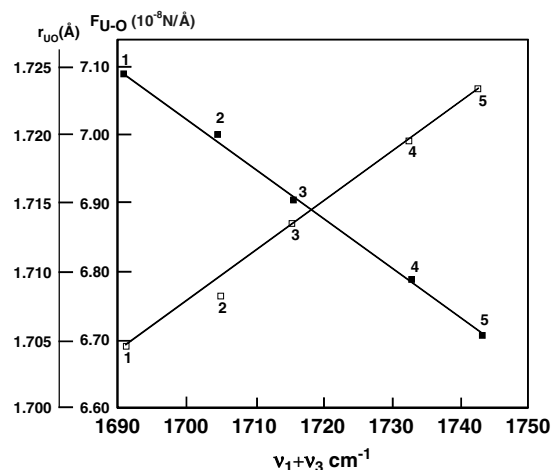


Figure 8. The relation between  $r_{U-O}$  and  $F_{U-O}$  vs  $v_1 + v_3$ .

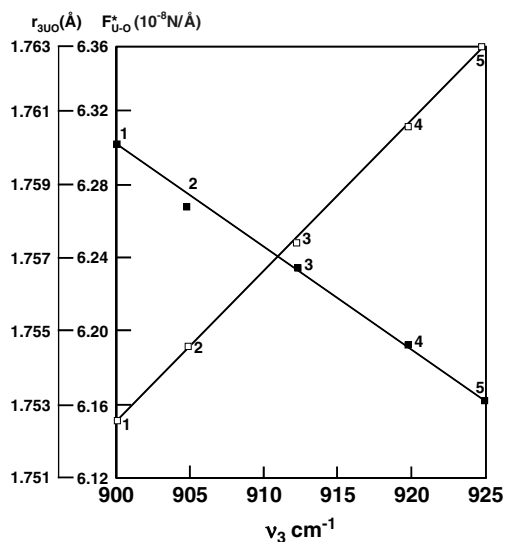
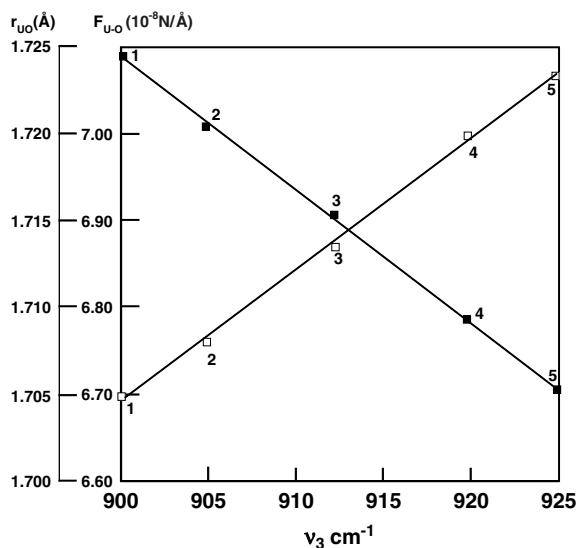


Figure 9. The relation between  $r_{U-O}$  and  $F_{U-O}$  vs  $v_3$ .

force constant of the U–O bond (Figs 8–10). There is also a straight line relationship between  $r_{U-O}$  and the  $p$ -substituent, Hamett's constant ( $\sigma^R$ ) with negative slope, i.e. the higher the value of  $\sigma^R$ , the lower  $r_{U-O}$  and the higher the force constant of the U–O bond (Fig. 11). Also, plotting of  $r_1$ ,  $r_2$ ,  $r_3$  and  $r_t$  (bond distance,  $r_{U-O}$ ) versus  $v_3$  gives straight lines with increase in the value of  $v_3$  and decrease in  $r_{U-O}$  (Fig. 12). Our results also showed an inverse relationship between  $v_3$  and  $r_{U-O}$ . This can be explained: the electron-withdrawing  $p$ -substitute increases the positive charge on the  $UO_2^{2+}$  leading to an increase in  $v_3$  and  $F_{U-O}$  and subsequently a decrease in  $r_{U-O}$ . Accordingly,  $r_{U-O}$  values can be arranged in the order:  $p-OCH_3 > p-CH_3 > H > p-Br > p-NO_2$ , consistent with the values of their  $\sigma^R$ .

Perhaps new light can be shed on the problem by looking at the values of  $r_1$ ,  $r_2$  and  $r_3$  from a different point of



**Figure 10.** The relation between  $r_{3\text{U-O}}$  and  $F_{\text{U-O}}^*$  vs  $\nu_3$ .

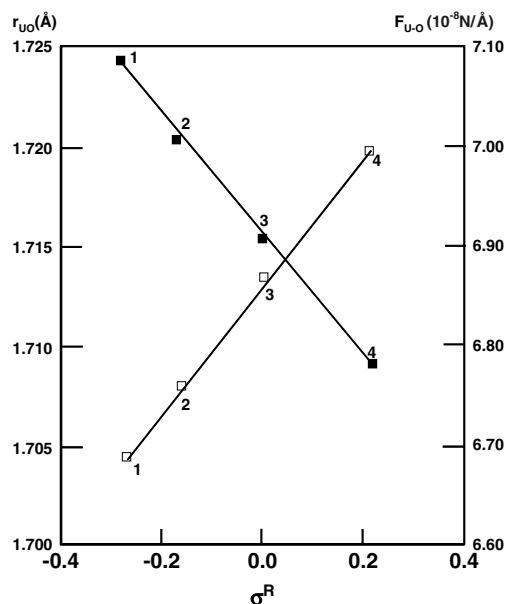


**Figure 11.** The variation of  $p$ -substituted Hammett's with (a)  $r_{\text{U-O}}$  (Å) and (b)  $F_{\text{U-O}}$  ( $10^{-8}$  N/Å).

view. It might be worthwhile to focus attention on their normalized differences. Thus a new relationship between them with respect to  $r_t$  (Table 4) was determined by global error, which shows that the validity is in the sequence:  $\sqrt{(r_3 - r_t)^2} > \sqrt{(r_1 - r_t)^2} > \sqrt{(r_2 - r_t)^2}$ .

### Stereochemistry and the structure of the complexes

Allyl propenyl-2-(4-derivatives phenylazo)butan-3-one ( $\text{HL}_n$ ) react with  $\text{UO}_2(\text{CH}_3\text{COO})_2 \cdot 2\text{H}_2\text{O}$  (molar ratio 2:1 in DMF)

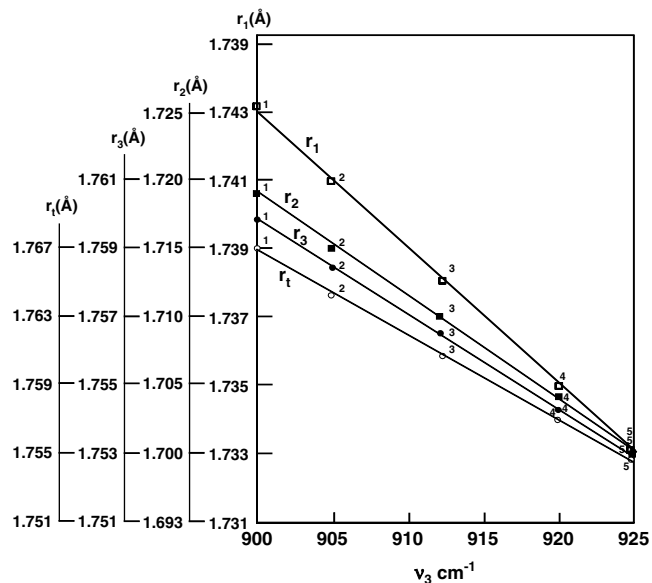


**Figure 12.** The relation between: (1)  $r_1$  vs  $\nu_3$ ; (2)  $r_2$  vs  $\nu_3$ ; (3)  $r_3$  vs  $\nu_3$ ; and (4)  $r_t$  vs  $\nu_3$ .

forming  $[\text{UO}_2(\text{HL}_n)_2 \cdot (\text{OAc})_2]_n$  stoichiometry with the neutral bidentate nature of the ligand and monodentate acetate groups; thus it is revealed that the coordination number of  $\text{UO}_2(\text{VI})$  is 8 in these complexes<sup>31</sup> [Fig. 1(b)]. The proposed structures of the polymer complexes are given in Fig. 1.

It is well established<sup>26</sup> that the uranyl ion possesses planar hexagonal structure with two oxygen atoms in the axial position. In the present complexes, two ligand units and two acetate molecules remain in the equatorial plane. It is also suggested that the two acetate molecules remain in the *trans*-position.

### Force constant, $F_{\text{U-O}}$ , and bond lengths, $R_{\text{U-O}}$ , of the uranyl polymer complexes

Owing to small scattering power of the oxygen atoms, reports of the determination of U–O bond length of some uranyl complexes by X-ray study are scanty. From infrared spectra, the stretching and interaction force constants in the present complexes have been calculated.<sup>3,26,27</sup> The results are in turn used to evaluate the U–O bond distances using the El-Sonbati equation,<sup>31</sup> Badger's formula<sup>32</sup> and Jones's equation.<sup>33,34</sup> The values are given in Table 4 and such a report is also found for other uranyl complexes.<sup>25,27,30,33,34</sup> The variation of bond length in the complexes is due to presence of electron-releasing or electron-withdrawing substituents in the equatorial position.

### CONCLUSION

From the overall studies presented,  $\text{HL}_n$  behaves as a chelating bidentate neutral ligand, bonding through two

oxygen atoms. The ligands have several isomers which are probably involved in coordination towards metal ions. The possible structures of the coordination compounds were determined in order to verify that the experimental structures were stable. Two different types of coordination compounds are suggested. In the first type, the ligand coordinates as a chelate through two carbonyl oxygen atoms as a bidentate. The second type of coordination behaves as bidentate through the (N=N) and oxygen atom of carbonyl group. The excellent agreement between calculated and experimental data supports the assignment suggested in the first type as in the present work.

It is of interest to compare these results with earlier findings. The definite absence of the N=N and the appearance of the bands implied NH and C=N after complexation. These bands were cited as evidence for the formation of the hydrazone system (Fig. 2) in the uranyl polymer complexes.

The analytical data of the uranyl polymer complexes are in a good agreement with 1:2 stoichiometries. The data also indicate the presence of acetate molecules (see Fig. 2).

In conclusion, the results arising from the present investigations confirm that the selected allyl propenyl-2-(4-derivatives phenylazo) butan-3-one (HL<sub>n</sub>) ligands are suitable for building a supramolecular structure. Moreover, since the azo and/or hydrazo compounds experience photochemical isomerization and are, therefore, of interest for applicative purposes,<sup>35</sup> the allyl propenyl-2-(4-derivatives phenylazo) butan-3-one (HL<sub>n</sub>) moiety are considered promising supramolecules that could be useful in molecular materials. Work is underway on the synthesis and characterization of further ruthenium, rhodium and vanadyl polymer compounds of this family of ligands and towards the development of the materials they produce. Further studies with the title ligand, using different metal ions, are in progress and will be published in due course.

## REFERENCES

- Atwood JL, Lehn J-M, Davies JED, Mociño DD, Vogtle F. *Comprehensive Supramolecular Chemistry*. Peragon Press: New York, 1996.
- Shoair AF, El-Bindary AA, El-Sonbati AZ, Younes RM. *Spectrochim. Acta Pt A* 2001; **57**: 1683.
- El-Sonbati AZ, El-Bindary AA, Diab MA. *Spectrochim. Acta Pt A* 2002; **59**: 443.
- Bruce DW, O'Hare D (eds). *Inorganic Materials*. Wiley: Chichester, 1992.
- Hemiton DE. *Inorg. Chem.* 1991; **30**: 1670.
- Issa RM, El-Bindary AA, El-Sonbati AZ, Kera HM. *Eur. Polym. J.* 2002; **38**: 561.
- Wills Jr. JN, Cook RB, Jankow R. *Anal. Chem.* 1982; **44**: 1228.
- Mubarak AT, El-Assiery SA. *Appl. Organomet. Chem.* 2004; **18**: 343.
- Mubarak AT. *Spectrochim. Acta Pt A* 2006; **65**: 0000.
- Selwood PW. *Magneto Chemistry*. Interscience: New York, 1956.
- El-Sonbati AZ, El-Bindary AA, Diab MA, El-Ela MA, Mazrouh SA. *Polym. Degrad. Stabil.* 1993; **42**: 1.
- El-Sonbati AZ, El-Bindary AA, Diab MA, Mazrouh SA. *Polymer* 1994; **35**: 647.
- El-Sonbati AZ, El-Bindary AA. *New Polymer. Matter.* 1996; **5**: 51.
- El-Sonbati AZ, El-Bindary AA, Rashed IG. *Spectrochim. Acta Pt A* 2002; **58**: 1411.
- Issa RM, El-Bindary AA, El-Sonbati AZ, Kera HM. *J. Inorg. Organometal. Polym.* 2003; **13**: 269.
- Pungor E. *Practical Guide to Instrumental Analysis*. CRC Press: Boca Raton, FL, 1995.
- Geary WJ. *Coord. Chem. Rev.* 1971; **7**: 81.
- Day JP, Venanzi LM. *J. Chem. Soc. A* 1966; 1363.
- Misra BB, Mohanty SR, Murti NVVS, Raychaudhri S. *Inorg. Chim. Acta* 1978; **28**: 275.
- Nishida Y, Kida S, Cremer S, Nakamoto N. *Inorg. Chim. Acta* 1981; **49**: 85.
- Levi L, Hubley CE. *Anal. Chem.* 1956; **28**: 1599.
- Fuson N, Lagrange G, Josien HL. *Spectrochim. Acta* 1960; **16**: 106.
- Nakanish K. *IR Absorbance Spectroscopy*. Holden Day: San Francisco, CA, 1962; 39.
- Mubarak AT, El-Sonbati AZ, El-Bindary AA. *Appl. Organomet. Chem.* 2004; **18**: 212.
- Hassib HB, Adel-Iatif SA. *Spectrochim. Acta A* 2003; **59**: 2425.
- El-Dissouky A, El-Bindary AA, El-Sonbati AZ, Hilali AS. *Spectrochim. Acta Pt A* 2001; **57**: 1163.
- El-Sonbati AZ, El-Dissouky A. *Transition Met. Chem.* 1986; **12**: 112.
- Rastogi VK, Pandey AN, Gupta SL, Saxena RC. *J. Pure Appl. Phys.* 1980; **18**: 379.
- Paolucci G, Marangoni G, Bandoli G, Clementi DA. *J. Chem. Soc. Dalton* 1980; 459.
- McGlynn SP, Smith JK, Neely WC. *J. Chem. Phys.* 1961; **35**: 105.
- El-Sonbati AZ. *Spectrosc. Lett.* 1997; **30**: 459.
- Badger RMN. *J. Chem. Phys.* 1935; **3**: 710.
- Jones LH. *Spectrochim. Acta* 1958; **10**: 395.
- Jones LH. *Spectrochim. Acta* 1959; **11**: 409.
- Sekka Z, Kang CS, Aust EF, Wegner G, Knoll W. *Chem. Mater.* 1995; **7**: 142.